Discrete Adjoint Optimization Framework for Unsteady Fluid-Structure Interaction Problems

Charanya Venkatesan-Crome
Rafael Palacios

Imperial College London

Department of Aeronautics

11 June 2020

Overview

1. Motivation
2. Technical Background
   - Primal Coupled FSI Solver
   - Discrete Adjoint Coupled FSI Solver
3. Numerical Results
   - Limit Cycle Oscillation of NACA 0012 Airfoil
   - Preliminary Gradient Validation
4. Conclusions

Why consider dynamic FSI optimization?

- Increased flexibility next generation aircraft necessitates FSI
- Static simulations informs baseline aerodynamic features, but dynamic events often size the structure
- Time-domain captures inherent instabilities and responses to external input (flutter, LCOs, gust loads, etc)

(a) Zephyr (Image Credit: Airbus)

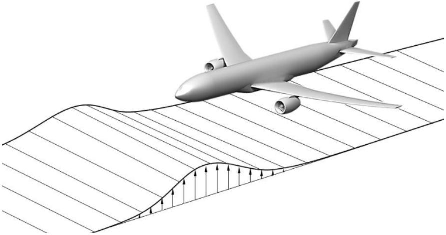

(b) Gust-Load Alleviation (Image Credit: Lancelot @ ICAST 2016)

Optimization Framework

- Built on native FSI solver in SU2
- Gradient based optimization for shape or material properties
- Leverages existing AD-based discrete adjoint solver for static problems
- CDiscAdjMultizoneDriver extended for unsteady problems
  - Supports multizone unsteady adjoint sensitivities not exclusive to FSI

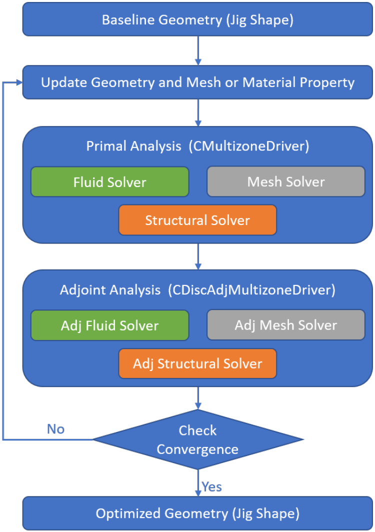

Primal Coupled FSI Solver

- Fluid Solver - RANS in ALE formulation

$$\frac{\partial \mathbf{w}}{\partial t} + \nabla \cdot \mathbf{F}^{\mathbf{c}}_{\mathbf{ALE}} - \nabla \cdot \mathbf{F}^{\mathbf{v}} - \mathbf{Q} = \mathbf{0}, \quad \mathbf{w} = \{\rho, \rho\mathbf{v}, \rho e\}^{\mathsf{T}}$$

$$\mathbf{F}^{\mathbf{c}}_{\mathbf{ALE}} = \left\{ \begin{array}{c} \rho(\mathbf{v} - \dot{\mathbf{z}}) \\ \rho\mathbf{v} \otimes (\mathbf{v} - \dot{\mathbf{z}}) + \bar{\bar{I}}p \\ \rho e(\mathbf{v} - \dot{\mathbf{z}}) + p\mathbf{v} \end{array} \right\}, \quad \mathbf{F}^{\mathbf{v}} = \left\{ \begin{array}{c} \mathbf{0} \\ \bar{\bar{\tau}} \\ \bar{\bar{\tau}} \cdot \mathbf{v} + \mu C_p \nabla T \end{array} \right\}$$

- Structural Solver - Non-Linear Solid Mechanics

$$\underbrace{\int_v \boldsymbol{\sigma} : \delta\mathbf{d}\ dv}_{\text{Internal}} - \underbrace{\left(\int_v \mathbf{f} \cdot \delta\mathbf{u}\ dv + \int_{\partial v} \mathbf{t} \cdot \delta\mathbf{u}\ da \right)}_{\text{External}} + \underbrace{\int_v \rho\delta\ddot{\mathbf{u}}\ dv}_{\text{Inertial}} = \mathbf{0}$$

- Mesh Solver - Linear Elasticity

$$\tilde{\mathbf{K}}_m \mathbf{z} - \tilde{\mathbf{f}}(\mathbf{u}) = \mathbf{0}$$

- Continuity of tractions and displacements at interface

Unsteady FSI Discrete Adjoint Solver

- To derive the adjoint equations, the optimization problem is written in fixed-point iterators

$$
\begin{aligned}
\min_{\mathbf{a}} \quad & \frac{1}{N}\sum_{n=1}^{N} J^n(\mathbf{u}^n, \mathbf{w}^n, \mathbf{z}^n, \mathbf{a}) \\
\text{subject to} \quad & \mathbf{S}^n\left(\mathbf{u}^n, \mathbf{u}^{n-1}, \mathbf{w}^n, \mathbf{z}^n, \mathbf{a}\right) - \mathbf{u}^n = \mathbf{0}, \quad n = 1, ..., N, \\
& \mathbf{G}^n\left(\mathbf{w}^n, \mathbf{w}^{n-1}, \mathbf{w}^{n-2}, \mathbf{z}^n, \mathbf{z}^{n-1}, \mathbf{z}^{n-2}, \mathbf{a}\right) - \mathbf{w}^n = \mathbf{0}, \quad n = 1, ..., N, \\
& \mathbf{M}^n(\mathbf{u}^n, \mathbf{a}) - \mathbf{z}^n = \mathbf{0}, \quad n = 1, ..., N.
\end{aligned}
$$

Unsteady FSI Discrete Adjoint Equations

- Taking the Lagrangian and differentiating with respect to the design variables

$$
\begin{aligned}
\frac{\mathrm{d}L}{\mathrm{d}\mathbf{a}} = & \sum_{n=1}^{N} \left[\frac{1}{N} \frac{\partial J^n}{\partial \mathbf{a}} + \left(\bar{\mathbf{u}}^n\right)^\mathsf{T} \frac{\partial \mathbf{S}^n}{\partial \mathbf{a}} + \left(\bar{\mathbf{w}}^n\right)^\mathsf{T} \frac{\partial \mathbf{G}^n}{\partial \mathbf{a}} + \left(\bar{\mathbf{z}}^n\right)^\mathsf{T} \frac{\partial \mathbf{M}^n}{\partial \mathbf{a}} \right] \\
& + \sum_{n=1}^{N} \left[\frac{1}{N} \frac{\partial J^n}{\partial \mathbf{u}^n} + \sum_{i=n}^{n+1} \left[\left(\bar{\mathbf{u}}^i\right)^\mathsf{T} \frac{\partial \mathbf{S}^i}{\partial \mathbf{u}^n} \right] - \left(\bar{\mathbf{u}}^n\right)^\mathsf{T} + \left(\bar{\mathbf{z}}^n\right)^\mathsf{T} \frac{\partial \mathbf{M}^n}{\partial \mathbf{u}^n} \right] \frac{\mathrm{d}\mathbf{u}^n}{\mathrm{d}\mathbf{a}} \\
& + \sum_{n=1}^{N} \left[\frac{1}{N} \frac{\partial J^n}{\partial \mathbf{w}^n} + \left(\bar{\mathbf{u}}^n\right)^\mathsf{T} \frac{\partial \mathbf{S}^n}{\partial \mathbf{w}^n} + \sum_{i=n}^{n+2} \left[\left(\bar{\mathbf{w}}^i\right)^\mathsf{T} \frac{\partial \mathbf{G}^i}{\partial \mathbf{w}^n} \right] - \left(\bar{\mathbf{w}}^n\right)^\mathsf{T} \right] \frac{\mathrm{d}\mathbf{w}^n}{\mathrm{d}\mathbf{a}} \\
& + \sum_{n=1}^{N} \left[\frac{1}{N} \frac{\partial J^n}{\partial \mathbf{z}^n} + \left(\bar{\mathbf{u}}^n\right)^\mathsf{T} \frac{\partial \mathbf{S}^n}{\partial \mathbf{z}^n} + \sum_{i=n}^{n+2} \left[\left(\bar{\mathbf{w}}^i\right)^\mathsf{T} \frac{\partial \mathbf{G}^i}{\partial \mathbf{z}^n} \right] - \left(\bar{\mathbf{z}}^n\right)^\mathsf{T} \right] \frac{\mathrm{d}\mathbf{z}^n}{\mathrm{d}\mathbf{a}}
\end{aligned}
$$

Unsteady Fluid Discrete Adjoint Equations

- Expression for the gradient of J

$$\frac{\mathrm{d}J}{\mathrm{d}\mathbf{a}} = \frac{\mathrm{d}L}{\mathrm{d}\mathbf{a}} = \sum_{n=1}^{N} \left[\frac{1}{N} \frac{\partial J^n}{\partial \mathbf{a}} + \left(\bar{\mathbf{u}}^n\right)^\mathsf{T} \frac{\partial \mathbf{S}^n}{\partial \mathbf{a}} + \left(\bar{\mathbf{w}}^n\right)^\mathsf{T} \frac{\partial \mathbf{G}^n}{\partial \mathbf{a}} + \left(\bar{\mathbf{z}}^n\right)^\mathsf{T} \frac{\partial \mathbf{M}^n}{\partial \mathbf{a}} \right].$$

- Adjoint equations defined by

$$\left(\bar{\mathbf{u}}^n\right)^\mathsf{T} = \frac{1}{N} \frac{\partial J^n}{\partial \mathbf{u}^n} + \sum_{i=n}^{n+1} \left[\left(\bar{\mathbf{u}}^i\right)^\mathsf{T} \frac{\partial \mathbf{S}^i}{\partial \mathbf{u}^n} \right] + \left(\bar{\mathbf{z}}^n\right)^\mathsf{T} \frac{\partial \mathbf{M}^n}{\partial \mathbf{u}^n}, \quad n = N, ..., 1,$$

$$\left(\bar{\mathbf{w}}^n\right)^\mathsf{T} = \frac{1}{N} \frac{\partial J^n}{\partial \mathbf{w}^n} + \left(\bar{\mathbf{u}}^n\right)^\mathsf{T} \frac{\partial \mathbf{S}^n}{\partial \mathbf{w}^n} + \sum_{i=n}^{n+2} \left[\left(\bar{\mathbf{w}}^i\right)^\mathsf{T} \frac{\partial \mathbf{G}^i}{\partial \mathbf{w}^n} \right], \quad n = N, ..., 1,$$

$$\left(\bar{\mathbf{z}}^n\right)^\mathsf{T} = \frac{1}{N} \frac{\partial J^n}{\partial \mathbf{z}^n} + \left(\bar{\mathbf{u}}^n\right)^\mathsf{T} \frac{\partial \mathbf{S}^n}{\partial \mathbf{z}^n} + \sum_{i=n}^{n+2} \left[\left(\bar{\mathbf{w}}^i\right)^\mathsf{T} \frac{\partial \mathbf{G}^i}{\partial \mathbf{z}^n} \right], \quad n = N, ..., 1.$$

- CoDiPack [Sagebaum, 2017] for Algorithmic Differentiation

Numerical Results: FSI NACA 0012 Airfoil

- NACA 0012 airfoil at Mach 0.8 with angle of attack of 8°, inviscid flow
- Clamp at 20% chord, flexible airfoil with $E = 70\text{MPa}$
- Hyper elastic Neo-Hookean material model

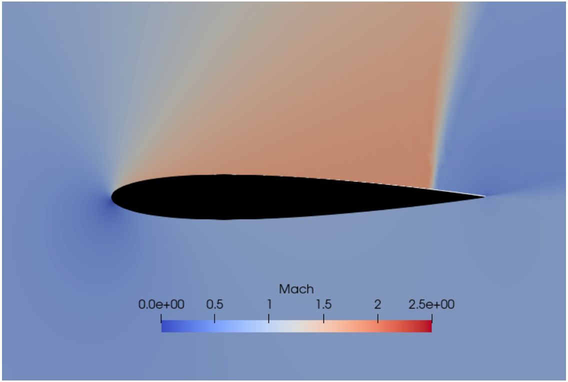

Numerical Results: FSI NACA 0012 Airfoil

A dynamic process:

1. Flexible airfoil leads to upward displacement of the trailing edge
2. Resulting shape of the airfoil further accentuates the aerodynamic loading to cause 20% upward displacement
3. Strengthened shock on the lower surface leads to a downward trailing edge displacement

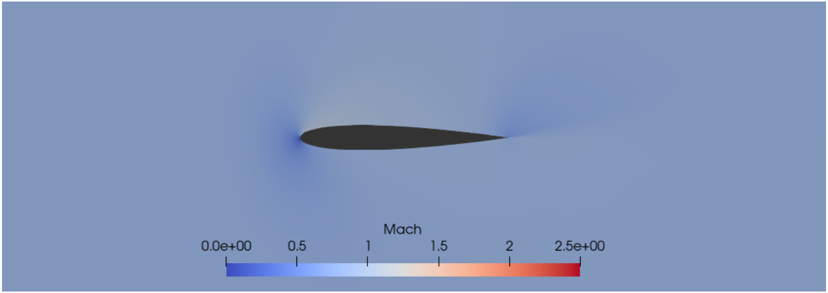

Numerical Results: FSI NACA 0012 Airfoil

A dynamic process:

1. Flexible airfoil leads to upward displacement of the trailing edge
2. Resulting shape of the airfoil further accentuates the aerodynamic loading to cause 20% upward displacement
3. Strengthened shock on the lower surface leads to a downward trailing edge displacement

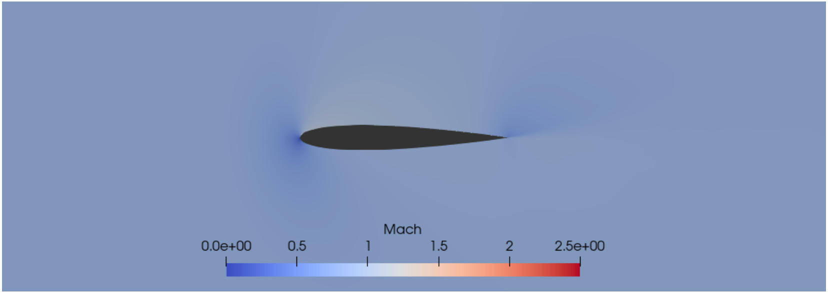

Numerical Results: FSI NACA 0012 Airfoil

A dynamic process:

1. Flexible airfoil leads to upward displacement of the trailing edge
2. Resulting shape of the airfoil further accentuates the aerodynamic loading to cause 20% upward displacement
3. Strengthened shock on the lower surface leads to a downward trailing edge displacement

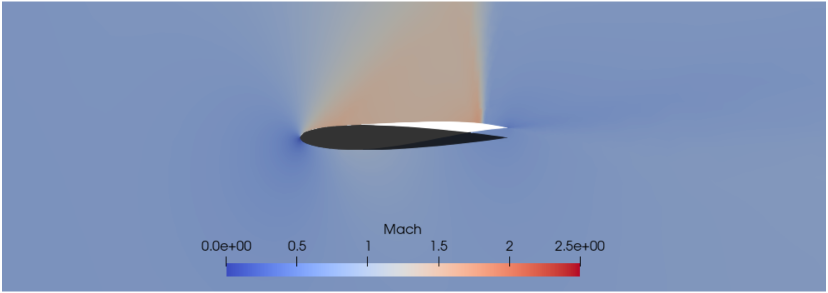

Numerical Results: FSI NACA 0012 Airfoil

A dynamic process:

1. Flexible airfoil leads to upward displacement of the trailing edge
2. Resulting shape of the airfoil further accentuates the aerodynamic loading to cause 20% upward displacement
3. Strengthened shock on the lower surface leads to a downward trailing edge displacement

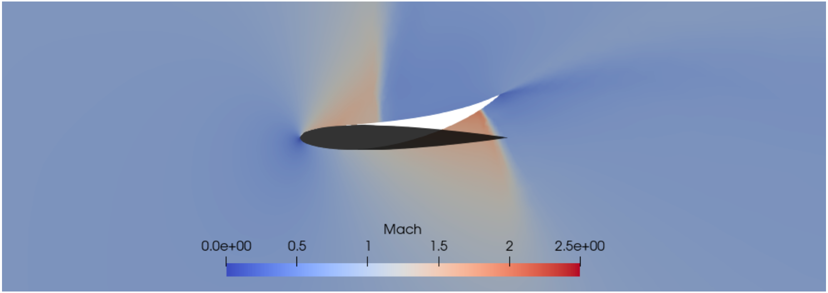

Numerical Results: FSI NACA 0012 Airfoil

A dynamic process:

1. Flexible airfoil leads to upward displacement of the trailing edge
2. Resulting shape of the airfoil further accentuates the aerodynamic loading to cause 20% upward displacement
3. Strengthened shock on the lower surface leads to a downward trailing edge displacement

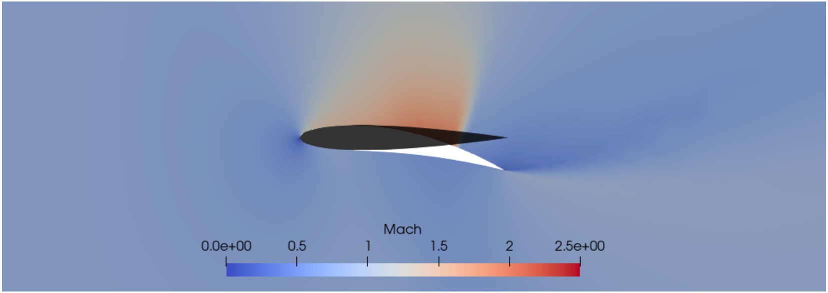

Numerical Results: FSI NACA 0012 Airfoil

- Undamped limit oscillations
- Tip displacements up to 38% chord
- Oscillating frequencies: tip displacement and lift at 11.3Hz

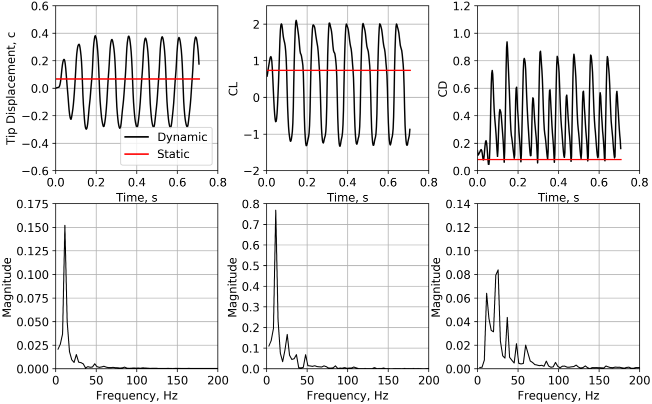

Numerical Results: FSI NACA 0012 Airfoil

- Gradient of average efficiency: $\frac{1}{T}\int_0^T \frac{C_L}{C_D}\mathrm{d}t$
- Design variables of FFD control points
- Sensitivities for the initial response up to 1% tip displacement
- Good agreement against finite differences using step size of 1mm/c

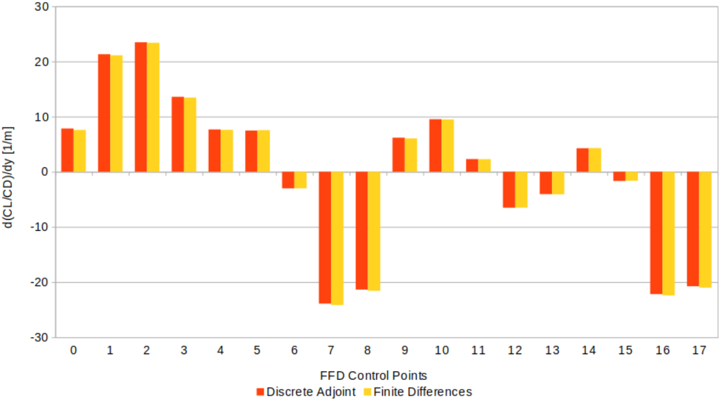

Conclusions

- Discrete adjoint methodology for time-domain FSI
- Shock-induced oscillations investigated in unsteady coupled FSI
- Preliminary gradient validation with small displacements
- Work in progress to extend to problems with geometric non-linearities
- Future work on optimal design for passive gust-load alleviation

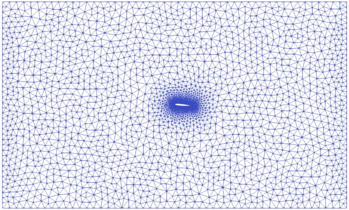

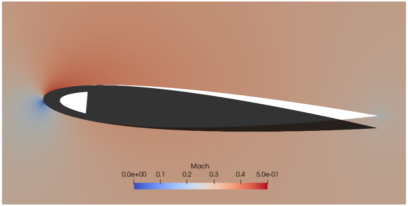

Conclusions

- Discrete adjoint methodology for time-domain FSI
- Shock-induced oscillations investigated in unsteady coupled FSI
- Preliminary gradient validation with small displacements
- Work in progress to extend to problems with geometric non-linearities
- Future work on optimal design for passive gust-load alleviation

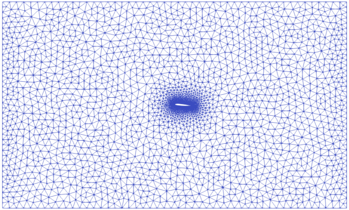

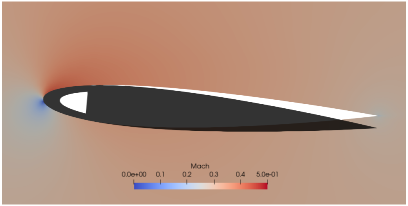

Discrete Adjoint Optimization Framework for Unsteady Fluid-Structure Interaction Problems

Charanya Venkatesan-Crome
Rafael Palacios

Imperial College London

Department of Aeronautics

11 June 2020